GEOFIZIKA VOL. 34 2017

DOI: 10.15233/gfz.2017.34.6
Professional paper
UDC 550.38

Magnetic susceptibility and natural gamma radioactivity as indirect proxies for characterization of sandstones and limestones of the Sabinas basin

José A. Batista Rodríguez[1], Joaquín A. Proenza Fernández[2], Antonio Rodríguez Vega[1], Felipe de Jesus López Saucedo[1] and Karla I. Cázares Carreón[1]

[1] Escuela Superior de Ingeniería, Universidad Autónoma de Coahuila, Coahuila, México

[2] Departament de Cristallografia, Mineralogia i Dipòsits Minerals, Facultat de Geologia, Universitat de Barcelona, Barcelona, 08028, Catalonia, Spain

Received 1 March 2017, in final form 14 April 2017

An analysis of magnetic susceptibility and natural gamma radioactivity is presented as indirect proxies of the characteristics of sandstones and limestones of the Sabinas basin. These rocks are located in the sedimentary sequence ranging from the Upper Jurassic to the Cretaceous. The magnetic susceptibility indicates changes in the magnetic composition of these rocks and suggests changes in their weathering degree. Ranges of values of magnetic susceptibility in sandstones and limestones allow classifying them into different groups, suggesting variability regarding conditions of origin and evolution. High values of magnetic susceptibility in limestones can be linked to sedimentation in anoxic or reducing environment, as well as with its siliciclastic content. The natural gamma radioactivity expressed in the contents of Th and relationships U / K and Th / U also suggest the degree of weathering of these rocks, mainly in the sandstones. These relations also highlight others characteristics in the sandstones related the probable provenance of sediments, its distance, degree of weathering and transport dynamics. Using the values of U / K ratio in the sandstones, it is possible to suggest the probable quartz-feldspar relationships. These ratio values classified rocks as arkose or quartzarenite, indicating the maturity of the sandstones. According to the U / K ratio values, most of these rocks which show little maturity are called arkose. Using the values of the Th / U ratio, it is possible to suggest the textures of quartzarenites, classifying them as rocks with fabric that is clast-supported or matrix-supported.

Keywords: magnetic susceptibility, natural gamma radioactivity, limestones, sandstones, Sabinas basin

1. Introduction

The Sabinas basin is located in the northeastern part of Mexico and has a thickness exceeding 5000 meters of sedimentary rocks deposited in a marine environment. This basin was formed during the early Mesozoic due to the opening

of the Gulf of Mexico (Fig. 1). Several marine transgressions and regressions occurred in this region during most of the Mesozoic Era. These last processes linked to the structural characteristics and tectonic evolution of the region, determined the sedimentation patterns. Those patterns changed from the Late Cretaceous when the Laramide orogeny (Late Cretaceous to Eocene) caused a tectonic uplift that obliterated the structure of the basin (Eguiluz de Antuñano, 2001). As a consequence, mainly sedimentary rocks (*e.g.* siliciclastic, carbonate and evaporite rocks) have originated, however igneous rocks formed as an addition in different geological environments (Eguiluz de Antuñano, 2001; González-Sánchez et al., 2007). Important accumulations of metallic and non-metallic ores, as well as hydrocarbons are associated with these rocks (Eguiluz de Antuñano, 2001; Corona-Esquivel et al., 2006; García-Alonso et al., 2011; González-Sánchez et al., 2007, 2017).

In this region, various geological, geophysical and geochemical surveys have been carried out mainly oriented to the exploration and prospecting of mineral deposits (Eguiluz de Antuñano, 2001; Pascacio-Toledo, 2001; Corona-Esquivel et al., 2006; González-Sánchez et al., 2007, 2017; García-Alonso et al., 2011).

Despite the number of surveys performed, the characteristics of some levels of sedimentary rocks related to the conditions of origin and evolution are still unknown. These characteristics determine their mineral composition, degree alteration and enrichment in organic matter. Several previous studies have demonstrated the potential of magnetic susceptibility (κ) and natural gamma radioactivity (NGR) to assess the compositions of sedimentary rocks which indicate their conditions of origin and evolution (Adams and Weaver, 1958; Clark, 1997; Ellwood et al., 2000; Hladil et al., 2006; Bábek et al., 2010).

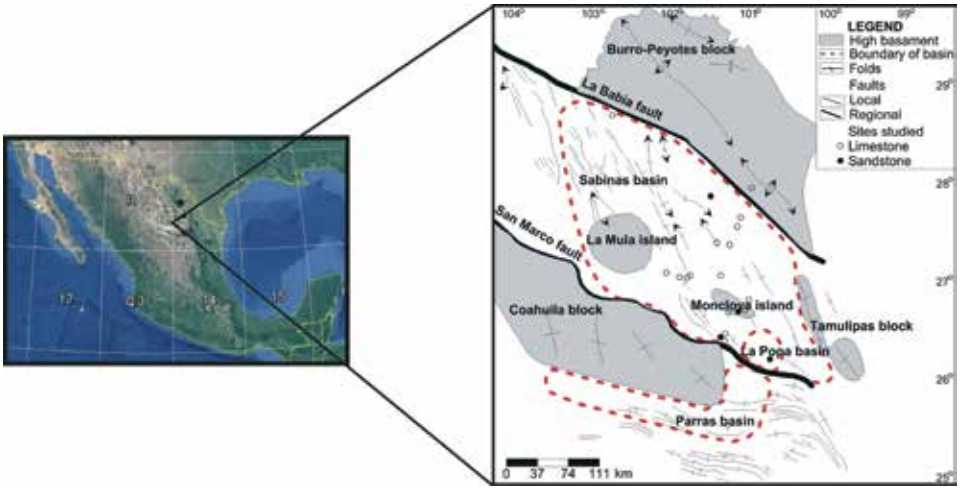

Figure 1. Locating of the study area (Sabinas basin). Structural configuration and tectonic characteristics of northeastern Mexico (modified of Chávez-Cabello et al., 2005).

The κ of rocks is related to the composition of magnetic minerals, mainly of iron oxides and hydroxides, iron sulfides and ferromagnesian silicates (Clark, 1997). These minerals may be present in accessory amounts in the sedimentary rocks (Boggs, 2009). Generally, these minerals are more abundant in siliciclastic sedimentary rocks than in carbonate rocks (Boggs, 2009), generating higher values of κ in the first type of rock that was mentioned (Clark, 1997). In the case of carbonate rocks, such as limestone, the κ is related to its impurities (Hladil et al., 2006).

The NGR is mainly due to the gamma radiation emitted by the radioactive isotope K40 and radioactive isotopes of the series of U (U^{238} and U^{235}) and the Th^{232} (Adams and Weaver, 1958). Therefore, the RGN is expressed in concentrations K (%), U (ppm) and Th (ppm). Most potassium occurs in rocks forming silicate minerals such as feldspars and micas, as well as, in some other common K-bearing minerals; *e.g.*, alunite and glauconite (Mittlefehldt, 1999). Th and U are constituents of the accessory minerals, such as zircon, monazite, allanite, xenotime, apatite and sphene, as well as, some minerals that have Th and U as a major constituent (*e.g.*, U in uraninite; Th in thorite and thorianite; both elements in uranothorite and uranothorianite) (Dickson and Scott, 1997).

The magnitudes of the κ and NGR in the rocks may vary due to geological processes that affect their mineralogical composition (Adams and Weaver, 1958). For example, the chemical weathering of rocks, causing decreases in content of U, because this radioactive element becomes mobile under supergene conditions (Bea, 1999). In these conditions the U migrates until finding the reducing barriers, such as organic matter zones. For this reason, high values of U can be registered in rocks enriched with organic matter (Lüning et al., 2004). The chemical weathering in sedimentary rocks also causes loss of K and increase of Th on the rocks, mainly associated with clays (Adams and Weaver, 1958). In these rocks, that process can also generate increases in κ caused by secondary minerals, such as magnetite and hematite (Clark, 1997).

In this research, an analysis of these two physical properties is presented, κ and NGR, on sandstones and limestones of the Sabinas basin with the aim of assessing the potential of both physical properties as indirect proxies to characterize these rocks, in order to evaluate its possible mineralogical composition, texture and alterations. Whereas most of the sedimentary infill of the basin is made up of siliciclastic and carbonate rocks (González-Sánchez et al., 2007, 2017) the rocks mentioned (sandstones and limestones) are selected for this study.

2. Geological setting

The Sabinas basin initially developed on the margin of the North America Craton during the opening of the Gulf of Mexico in the early Mesozoic Era. The high blocks of Tamaulipas (Tamaulipas arc and Burro-Peyotes block) and

Coahuila are the main paleotectonic and paleogeography limits of the basin (Fig. 1). This basin is a depression formed by a series of subsided blocks and some elevates to the northwest, which separate it from the Chihuahua basin. There are small uplifted blocks of basement within the Sabinas basin (La Mula and Monclova Island) (Eguiluz de Antuñano, 2001).

The Sabinas basin was developed through several evolutionary phases. The first phase was a long period of Triassic-Lower Jurassic magmatic-arc activity. In the second phase, a rupture of the lithosphere occurred, and in the third phase, the rift developed an association with the opening of the Gulf of Mexico (Eguiluz de Antuñano, 2001).

There are three main depositional supersequences in the Sabinas basin associated with the rift, drift and foreland stages of its evolution (Fig. 2). The first supersequence consists of conglomerates, salt interbedded with fine-grained red and green terrigenous rocks, anhydrite and carbonates. The stratigraphic position of this first cycle suggests a period of deposition during the Callovian (?)-lower Oxfordian (Goldhammer et al., 1991). These rocks mostly occur in the central part of basin. This group of rocks is representative of a transgressive-regressive cycle (Eguiluz de Antuñano, 2001).

The second supersequence represents the drift stage and it comprises several depositional cycles (II, III and IV): cycle II corresponds to upper Oxfordian to Berriasian age, cycle III to Valanginian to Aptian age and cycle IV to the Aptian-Cenomanian age.

Carbonated units in the base of the cycle II indicate a transgressive section that degrades up to coastal terrigenous facies (*e.g.*, La Casita Fm.) (Imlay, 1936).

During the Berriasian age (Early Cretaceous) terrigenous and clay-rich carbonates rocks with grain of varying sizes were deposited (*e.g.*, Taraises Fm.) (Imlay, 1936).

In another deposition cycle (cycle III), the basin subsidence and accumulation of sandstones and fine-grained terrigenous rocks continued. During the Hauterivian-Barremian age, it occurred a gradual change in sedimentation, and the formation of dolomite began with an increase in siltstone interbedded and reddish shales towards emerged continental areas represented by the Coahuila and Tamaulipas blocks (Murillo-Muñeton, 1999).

Later a new transgressive system was originated (cycle IV), in which the basal high-energy carbonates transitioned upwards into low-energy carbonates (*e.g.*, Cupidito Fm.) (Wilson and Pialli, 1977).

The deposition of basinal micritic limestones and shales began in the Albian age and continued until the Cenomanian age. In this period, an extensive carbonated platform prevailed in which carbonates and evaporites were deposited (*e.g.*, Aurora and Kiamichi Formations, as well as the Washita Group: Georgetown, Del Río and Buda Formations).

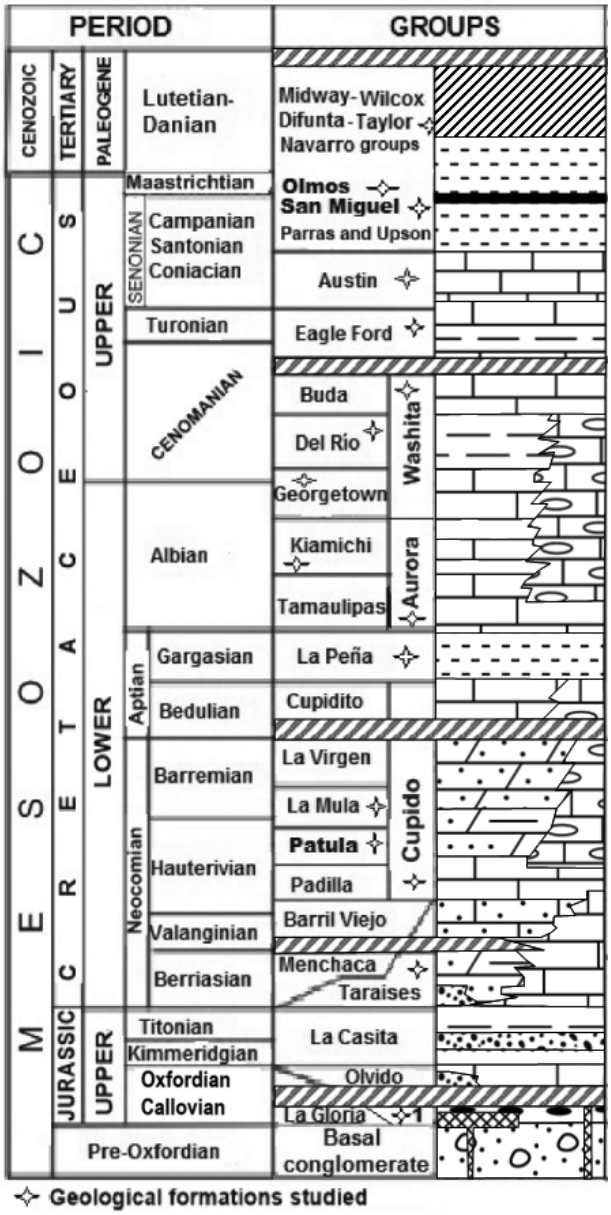

Figure 2. Generalized stratigraphic column of the Sabinas basin and surroundings (modified from Eguiluz de Antuñano, 2001). 1: Zuloaga Formation.

During most of the Late Cretaceous, the regressive and prograding sequences were originated (supersequence 3; cycle V), represented by regressive terrigenous strata deposited in a foreland basin setting (*e.g.*, Eagle Ford, Austin, San Miguel, Olmos and Escondido Formations) (Eguiluz de Antuñano, 2001).

3. Methodology

The study of κ and NGR in sandstones and limestones of the Sabinas basin was carried out in four stages. In the first stage, the fieldwork was planned and performed in 25 sites. Outcropping limestones were used for 16 sites and sandstones for 9. These rocks belong to geological formations of the Upper Jurassic to Cretaceous age (Fig. 2). In this research the κ was measured in outcrops of the two rocks taking 5 measurements at each point using a KT-10 Plus Magnetic Susceptibility Meter. The susceptibilimeter was placed directly on the rock, on a flat surface. The NGR was measured in outcrops using a RS-125 super gamma ray Spectrometer, which has 4 channels: Total gamma intensity ($I_{g,total}$ in μR / h), concentrations of potassium (K in %), uranium (U in ppm) and thorium (Th in ppm). Measurements of NGR were performed during 120 seconds at each point. The gamma ray Spectrometer was placed directly on the rock, on a flat surface.

The limestones range in age from the Upper Jurassic to the Late Cretaceous, representative of Zuloaga, Taraises, Cupido, La Mula, La Peña, Aurora and Kiamichi Formations, as well as the Washita Group and Eagle Ford and Austin Formations. The sandstones are principally located in the Pátula Formation with the Early Cretaceous age. These sandstones also belong to other geological formations of the Late Cretaceous, *e.g.* San Miguel and Olmos Formations and the Difunta Group (Fig. 2).

Samples were taken at each of the sites reaching a total of 305 samples (153 in limestones and 152 in sandstones; Tabs. 1 and 2).

Table 1. Descriptive statistics of the $\kappa \times 10^{-3}$ SI in sandstones and limestones of the Sabinas basin. N: number of outcrops and samples; SD: standard deviation; O+S: total of outcrops and samples.

Sandstones			
Measurements	Rank	Average	SD
Outcrops. $N = 9$	0.008–0.98	0.13	0.10
Samples. $N = 152$	0.001–0.61	0.08	0.05
O+S	0.001–0.98	0.09	0.08
Limestones			
Measurements	Rank	Average	SD
Outcrops. $N = 16$	0.001–0.47	0.071	0.05
Samples. $N = 153$	0.001–0.42	0.047	0.05
O+S	0.001–0.47	0.057	0.05

Table 2. Descriptive statistics of the NGR in sandstones of the Sabinas basin. A: average.

Measurements	$I_{g,total}$ (mR/h)			K (%)			U (ppm)			Th (ppm)		
	Range	A	SD	Range	A	SD	Range	A	SD	Range	A	SD
Outcrops. $N = 9$	5.1–23	12	4.7	1–9	3.8	2	0–7.7	2.6	1.6	4.1–36	15	5.6

During the second stage, the samples were prepared. Initially first were cut, creating flat surfaces in which the κ and NGR were measured placing the susceptibilimeter and spectrometer directly on these surfaces. Then, thin sections were prepared and described to assess the nature of the behavior of both physical properties, *i.e.*, determine the main minerals that determine the magnitudes obtained.

Measurements of NGR in the laboratory were carried out on samples having smaller rock volumes than in the outcrops. Therefore, the values of NGR obtained were only used to determine relationships between variables of the NGR ($I_{g,total}$, K, U and Th) and between these and κ. Such measurements were also used to determine changes in this physical property in the samples and to suggest the causes of these changes.

In the third stage, the statistical processing of the measurements data of both physical properties was carried out. In this processing the mean, variance, and maximum and minimum values were calculated, as well as histograms and correction matrix. In the final stage, the behavior of the physical properties and their probable causes were valued, according to the field descriptions and the analysis of thin sections.

4. Results

4.1. Characteristics of sandstones from analysis of κ and NGR

In sandstones, the highest values of both physical properties are recorded, however sometimes their range overlaps with limestones, mainly in κ (Tabs. 1 and 2). In these cases, the κ suggests similar contents of magnetic minerals. The ranges of κ indicate that some sandstones and limestones have high contents of paramagnetic minerals or at least medium-low contents of ferromagnetic minerals, according to Clark (1997). These minerals could be mainly iron oxides and hydroxides (*e.g.* magnetite, ilmenite, hematite and goethite), iron-rich silicates (*e.g.* mica, chlorite, epidote and titanite) and iron sulphides (*e.g.* pyrite and chalcopyrite) considering the typical composition of sedimentary rocks (Boggs, 2009). Previous studies in the Sabinas basin indicate that the sandstones are principally composed by quartz and feldspars, as well as by iron oxides, clays and carbonates in their matrix. They also have accessory minerals such as biotite, muscovite and zircon (Krutak, 1965; Ocampo-Díaz et al., 2014).

Figure 3. Outcrops of limestones (*A* and *B*) and sandstones (*C* and *D*). N indicate nodules of iron oxides.

The samples of sandstones and limestones have lower values of κ than those obtained in their outcrops. This difference suggests the differing formation of magnetic minerals during the weathering of the rocks (Fig. 3). Particularly in limestones, there is less difference between the two types of measurements (field and laboratory), showing less influence of this weathering process on the values of κ.

The behavior of the NGR in sandstones outcrops also suggests heterogeneity in their mineralogical composition. This physical property shows high variations of the total gamma intensity (×), which is mainly due to the contents of Th and also to K (Fig. 4). Most $I_{g,total} > 15$ μR / h values are obtained in green, yellow, gray and reddish fine-grained sandstones. The field work revealed that these rocks are very weathered (Fig. 3). Results of research in other regions indicate that this process can generate secondary minerals rich in Th and K (*e.g.* clays), due to the degradation of feldspars and micas (Gbadebo, 2011; Schuler et al., 2011).

Lower values of NGR are recorded in red sandstones characterized by being more compact, hard, and of middle and coarse grains, which are apparently less affected by chemical weathering.

Correlation matrices of the variables that define the NGR in outcrops and samples are presented (Tab. 3). These are calculated using a significance level of 0.05. In these matrices, significant relationships are evident between the variables (Correlation coefficients greater than 0.34) that are related to the chemical weathering described above and to the compositional variations of these rocks.

Table 3. Correlation matrix of NGR in sandstones of the Sabinas basin.

Samples				
	$I_{g,total}$	K	U	Th
$I_{g,total}$	1			
K	0.43	1		
U	0.29	–0.34	1	
Th	0.58	0.12	–0.36	1
Outcrops				
	$I_{g,total}$	K	U	Th
$I_{g,total}$	1			
K	0.94	1		
U	0.60	0.51	1	
Th	0.78	0.60	0.2	1

4.2. Characteristics of limestones from analysis of κ and NGR

Limestones and sandstones differ considerably in their values of κ and NGR. In limestones, the values of κ next to 1×10^{-3} SI (Tab. 1) indicate small amounts of paramagnetic and ferromagnetic minerals; for example, iron sulphides (pyrite) and iron oxides (magnetite). These minerals probably formed during the enrichment of organic matter that is present in most of these limestones in the region (Eguiluz de Antuñano, 2001; González-Sánchez et al., 2007). The accumulation of organic matter can originate iron sulphides, such as pyrite (Merinero et al., 2010). Later, this mineral can undergo an oxidation process and originate iron oxides; for example, magnetite (Hladil et al., 2006). Some limestones of the region show iron nodules (Fig. 3) indicating the process described.

The analysis of the NGR indicates that these rocks have high variability in Th and U concentrations (Tab. 2), suggesting great change in their composition, mainly represented by clay minerals and organic matter. The organic matter is likely related to the U concentrations.

A correlation matrix of the variables that define the NGR and κ in limestones samples was presented (Tab. 4). The significant relationships between the

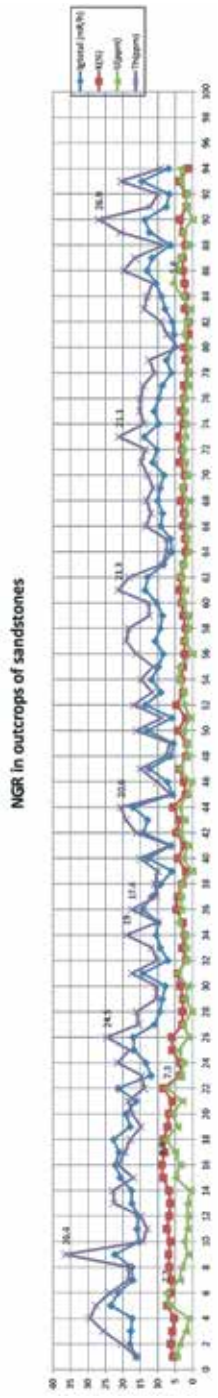

Figure 4. Variations of NGR in sandstones of the Sabinas basin.

variables (Correlation coefficients greater than 0.3) also are related to the compositional variations of these rocks.

Table 4. Correlation matrix of NGR and κ in samples of limestones.

	κ	$I_{g,total}$	K	U	Th
κ	1				
$I_{g,total}$	0.26	1			
K	0.15	0.30	1		
U	0	0.33	–0.21	1	
Th	0.16	0.54	0.06	–0.41	1

5. Discussion

5.1. Sandstones

Based on the values of κ the studied sandstones can be divided into three groups (Figs. 5 and 6). This classification indicates a high degree of heterogeneity in their comsposition of magnetic minerals.

Most of these sandstones belong to group 1 which is characterized by low values of κ indicating a very low content of magnetic minerals (paramagnetic and ferromagnetic minerals). Less than 40% of the measurements belong to groups 2 and 3, which include sandstones with high contents of paramagnetic minerals and / or small contents of ferromagnetic minerals. Most sandstones of the groups 2 and 3 belong to the Pátula Formation (Fig. 3).

In outcrops, over 60% of the measurements are located in the second group whereas those in samples have over 70% in the group 1. This difference could be linked to weathering on these rocks (Fig. 3). During this process, iron-rich clays are formed due to degradation of feldspars and micas (*e.g.* illite and kaolinite), as well as iron oxides and hydroxides (*e.g.* hematite and goethite).

Because the measurements of κ in the sandstones samples were carried out in a not-weathered surface, the primary paramagnetic and ferromagnetic minerals are directly related to the recorded values in groups 2

and 3 of these samples (Figs. 5 and 6). The analysis of thin sections indicate that these minerals are mainly in the matrix or cement of these rocks (Fig. 7). This analysis shows iron oxides and hydroxides (magnetite, hematite and goethite) cementing clasts of quartz and feldspars, as well as iron oxides surrounded by iron hydroxides.

The above results suggest dividing the magnetic minerals of these sandstones in two groups: primary and secondary minerals, and the latter originating from the weathering of these rocks.

Comparing the values of κ in the samples of red sandstones Ar-6 and Ar-9 (Fig. 8) with the thin sections A (Ar-9) and B (Ar-6) of Fig. 7, it is evident that the Ar-9 sample with higher values of κ has more ferruginous cement. This comparison suggests a direct relationship between κ and the amount of ferruginous cement in these sandstones.

The values of κ are related to the colorations of sandstones (Fig. 8).

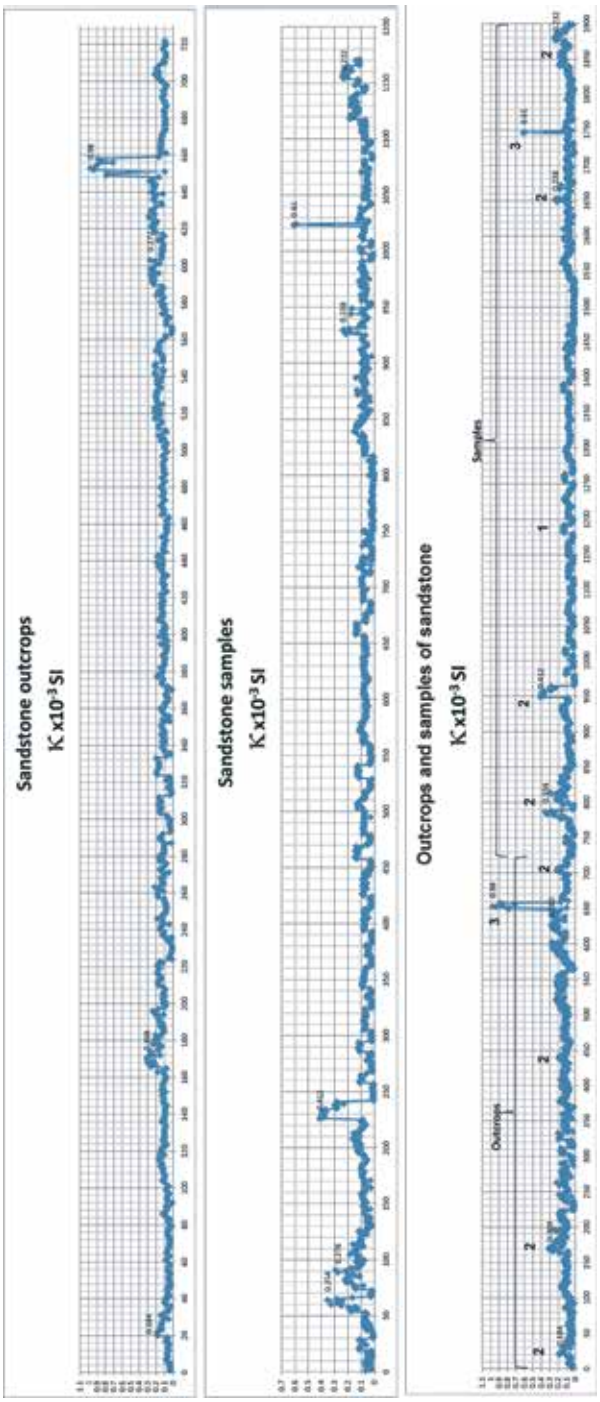

Figure 5. Variations of κ in sandstones of the Sabinas basin.

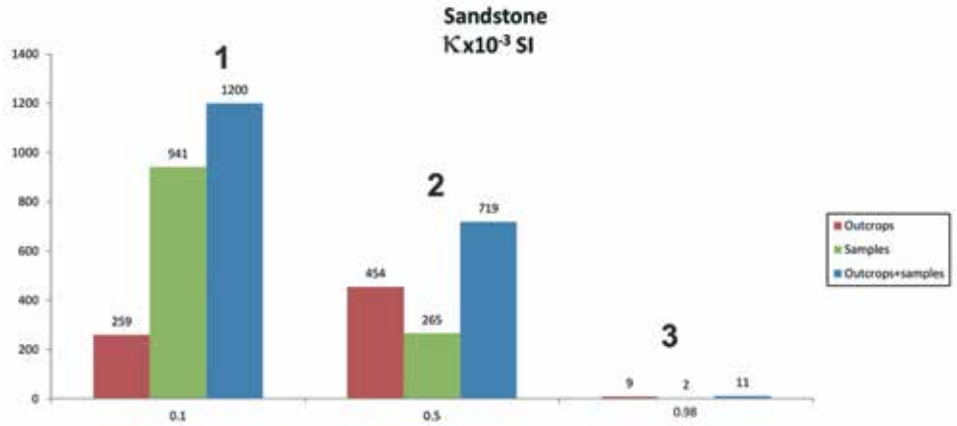

Figure 6. Histogram of κ in sandstones of the Sabinas basin. 1, 2 and 3 indicate groups of sandstones.

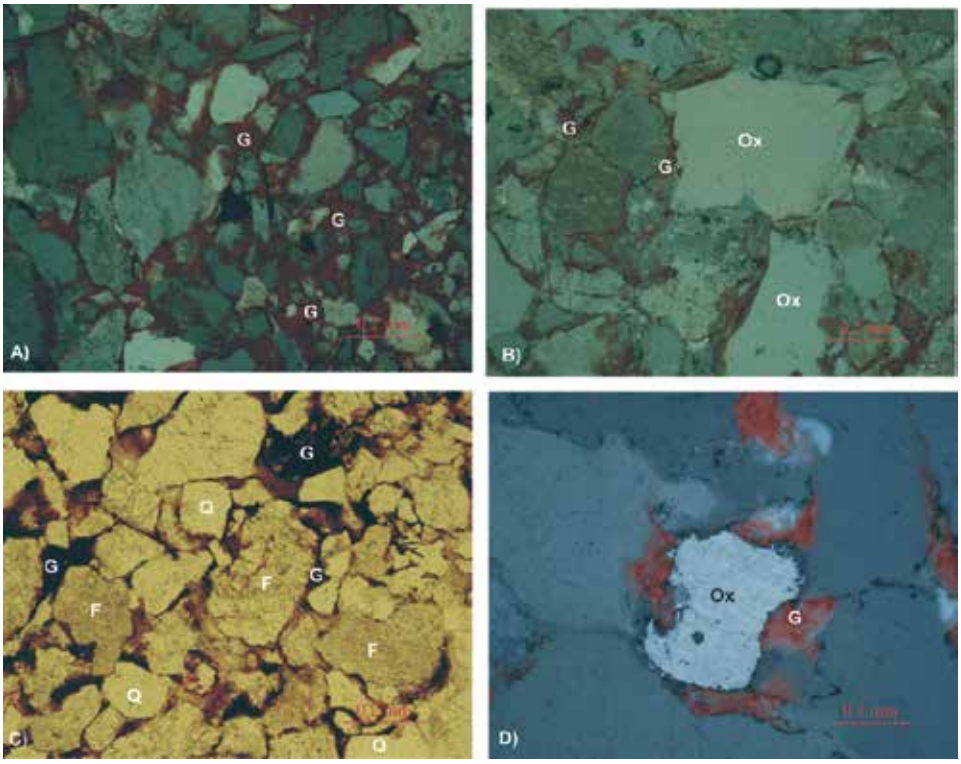

Figure 7. Thin sections in samples of red sandstones of the Pátula Formation. *A)* Reflected light (RL) with analyzer (*A*): goethite (G; red color) cementing clasts of quartz and feldspar. *B*) RL without analyzer (WA): iron oxides (Ox; gray color indicates magnetite and hematite). *C*) Transmitted light (TL) WA: potassium feldspar (F; dirty light color) and quartz (Q; clean light color) surrounded by goethite. *D*) RL A: iron oxides (Ox: magnetite and hematite) surrounded by goethite (red color).

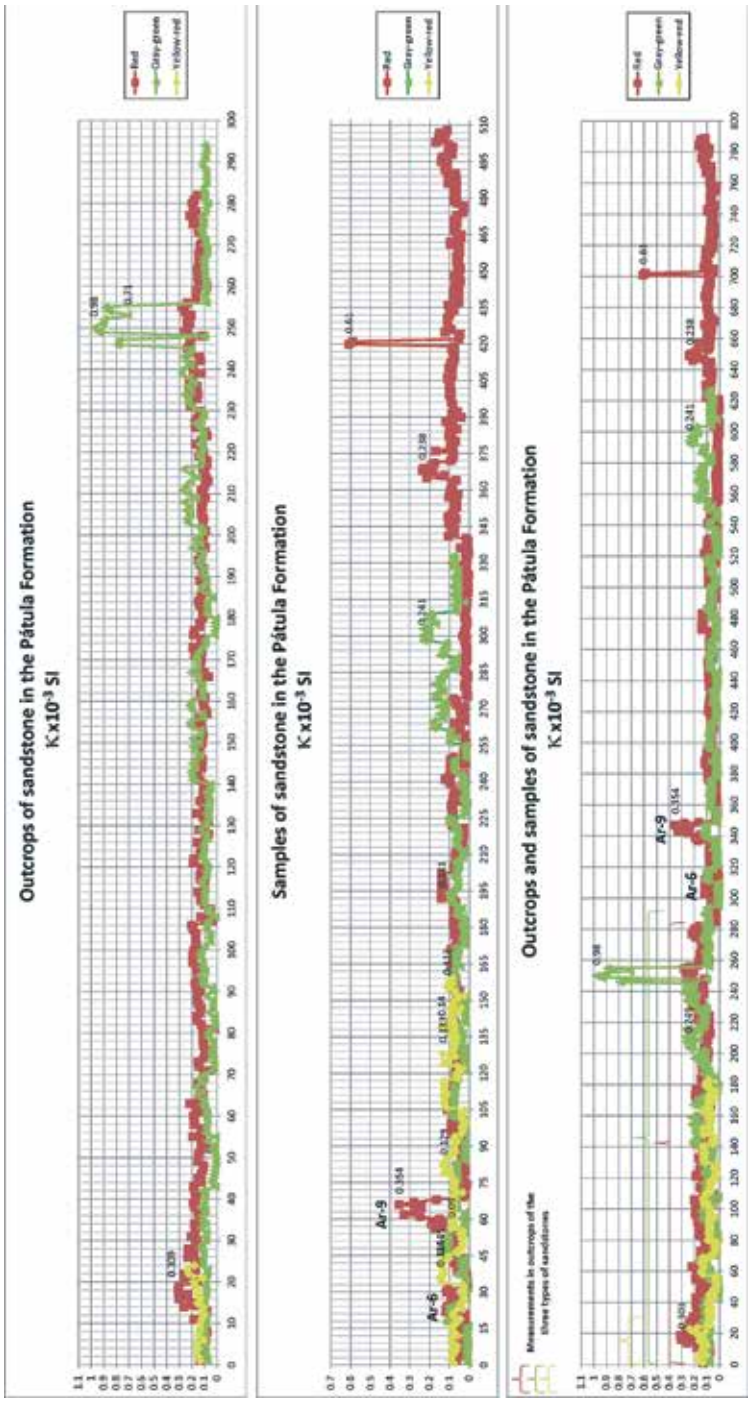

Figure 8. Variations of κ in sandstones of the Pátula Formation.

Generally, the outcrops of red sandstones have the highest values of κ indicating high concentrations of magnetic minerals. However, some outcrops of greenish gray sandstones exhibit higher concentrations of magnetic minerals, which are likely to be mainly of secondary origin (see graphics of outcrops in Fig. 8). In addition, the samples of red sandstones have the highest concentrations of magnetic minerals, mainly related to its matrix (see graphics of samples in Fig. 8). The analysis of κ in sandstones suggests using this physical property as indirect proxy to characterize its contents of magnetic mineral and texture.

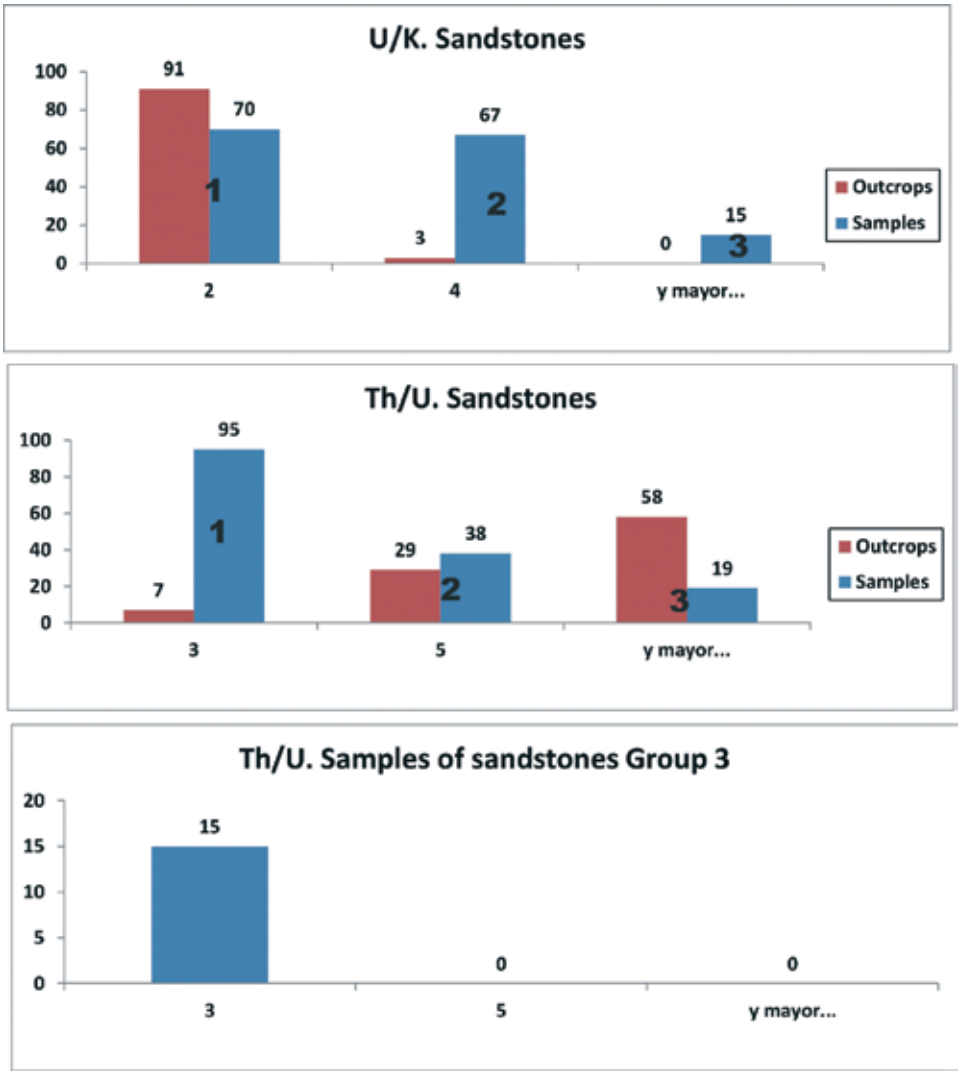

Figure 9. Histograms of U / K and Th / U ratios in sandstones of the Sabinas basin. 1, 2 and 3 indicate groups of sandstones.

Ratios between the radioelements (*e.g.* U / K and Th / U ratios) can reveal different characteristics of sedimentary rocks related to the supply areas (composition and weathering of rocks) and weathering and transportation of sediments (Adams and Weaver, 1958; Banerjee and Banerjee, 2010; Zand-Moghadam et al., 2013). In sandstones outcrops of the Sabinas basin, 99% of the values of U / K ratio are below 2 (Fig. 9). These values can indicate the intense process of weathering in these rocks. That is, most sandstones have high values of K and very low of U. This relationship occurs because U is more susceptible than K to migration during weathering of rocks (Dickson and Scott, 1997). Considering research results in other regions (Zand-Moghadam et al., 2013) state that the U / Th ratio also reveals such weathering processes because the majority of its values are greater than 4. This ratio can also indicate the degree of heterogeneity in the provenance of the sediments forming the detrital sedimentary rocks, as well as their depositional conditions (Adams and Weaver, 1958; Banerjee and Banerjee, 2010).

40% of the sandstones samples have values of Th / U > 4 (Fig. 9) suggesting that these rocks are composed of a mixture of sediments from different source areas. The Th / U ratio being greater 4 also suggests deposition oxidizing conditions in the basin where these sandstones were formed. The latter is a characteristic of the Pátula Formation (Ocampo-Díaz et al., 2014), to which most of the samples analyzed belong.

These sandstones also can be classified into three groups according to the values of the U / K ratio obtained in the samples (Fig. 9), considering that U can be related to the contents of silica and the K with the potassium feldspars principally (Mittle-fehldt, 1999; Dickson and Scott, 1997). Group 1: sandstones with high contents of feldspars and low content of quartz (U / K ≤ 2); Group 2: sandstones with relatively similar amounts of quartz and feldspars (U / K 2 to 4); Group 3: sandstones with high contents of quartz and low content of feldspars (U / K ≥ 4). In group 3 few samples of sandstones are included whereas 50% of the samples belong to group 1. Group 1 is characterized by higher amounts of K relative to U, unlike groups 2 and 3. Based on the classification, the detritus of the sandstones of group 3 is considered to come from nearby sources of granitic rocks with little chemical weathering. Many types of feldspar in these sandstones indicate a low degree of chemical weathering of rocks and little transport of detritus (Dickson and Scott, 1997). Probably the detritus of sandstones group 2 was supplied by rocks little enriched in feldspars rather than the rocks that provided the detritus of the sandstones in group 1. If the detritus of the sandstones belonging to groups 1 and 2 come from the same source areas, then the rocks of the source areas of group 2 show higher chemical weathering, and / or the detritus had greater transport causing a decrease of K contents (Dickson and Scott, 1997). In group 3, it is possible that the sandstones possess very weathered detritus or that this have been originated in different source areas to the two previous groups are included. This analysis suggests the probable heterogeneity in the composition of the rocks in the sources areas of the detritus, as well as their distances, transport conditions and intensity of weathering.

Considering the proposed previous classification, also suggests that most of the sandstones samples can be classified as arkose indicating little maturity in this rock. This proposal is consistent with the results of previous petrographic studies in the geological formation, which was identified as Pátula Arkose (Krutak, 1965). This classification also reveals that in this geological formation there are sandstones that can be classified as quartzarenite showing a high degree of maturity according to the classification of Tucker (2003).

Using the Th / U ratio, it is possible to suggest characterize the texture of group 3 sandstones assuming that Th contents are mainly related to its matrix and the U contents with their clasts. All samples of this group have values of Th / U ratio less than 3 (Fig. 9) indicating increases of U relative to Th probably related to sandstones with many quartz clasts and little matrix, *i.e.* a rock with clast-supported texture, considering the classification of Tucker (2003).

The analysis of both relationships between the radioelements (U / K and Th / U ratios) suggests the possibility of using these relationships as indirect proxy to reveals different stages of development of the weathering in the source areas and the same sandstones. Both ratios also are considered as proxy for classify the sandstones according to their relationship of quartz-feldspar and texture.

In the correlation matrix of the samples of sandstones (Tab. 3), the $I_{g,total}$ mainly depends on Th and K concentrations. The Th concentration seems to be associated mainly with the rock matrix, as is the K concentration, although the latter radioelement could also be related to feldspar clasts. Negative relations between U and the two radioelements (K and Th) indicate the bonding of U with different minerals other than thorium and potassium-bearing probably quartz.

In the correlation matrix of outcrops (Tab. 3), other relations between the variables are observed. In this case, the $I_{g,total}$ depends on the three radioelements and these in turn are interrelated positively. The observed relationships between radioelements can be related with clays (*e.g.* illite) originated by weathering of the sandstones.

5.2. Limestones

The composition, environment of formation and degree of alteration in the limestones also are revealed from the analysis of κ and NGR. Large differences in the values and variations of the measurements of κ in outcrops and samples are observed (Fig. 10). Using these differences can be possible to classify the limestones into four groups, each of which predominates in geological formations (noted at the top left of Fig. 10). The patterns of the groups are different in outcrops and samples; however, these groups are best defined by measurements of the samples. The differences reveal the presence of magnetic minerals caused by the weathering of rocks. In the first group the limestones belong mainly to the Aurora Formation, as well as to the La Mula, La

Peña, Kiamichi, Eagle Ford and Austin Formations (Fig. 2). This group is characterized by low values and little variations of κ ($\leq 0.05 \times 10^{-3}$ SI). The latter indicates little heterogeneity in the magnetic composition of limestones that integrate the stratigraphic sequence of these geological formations, suggesting little change in the formation environment and evolution of these rocks in the Sabinas basin. According to the ages of these geological formations, it is possible to define the intervals of deposition with these characteristics (Fig. 2), located from the Lower Cretaceous (Hauterivian) to Upper Cretaceous (Santonian).

Group 2 consists mainly of the Cupido Formation. In this group some measurements also appear belonging to the Aurora and

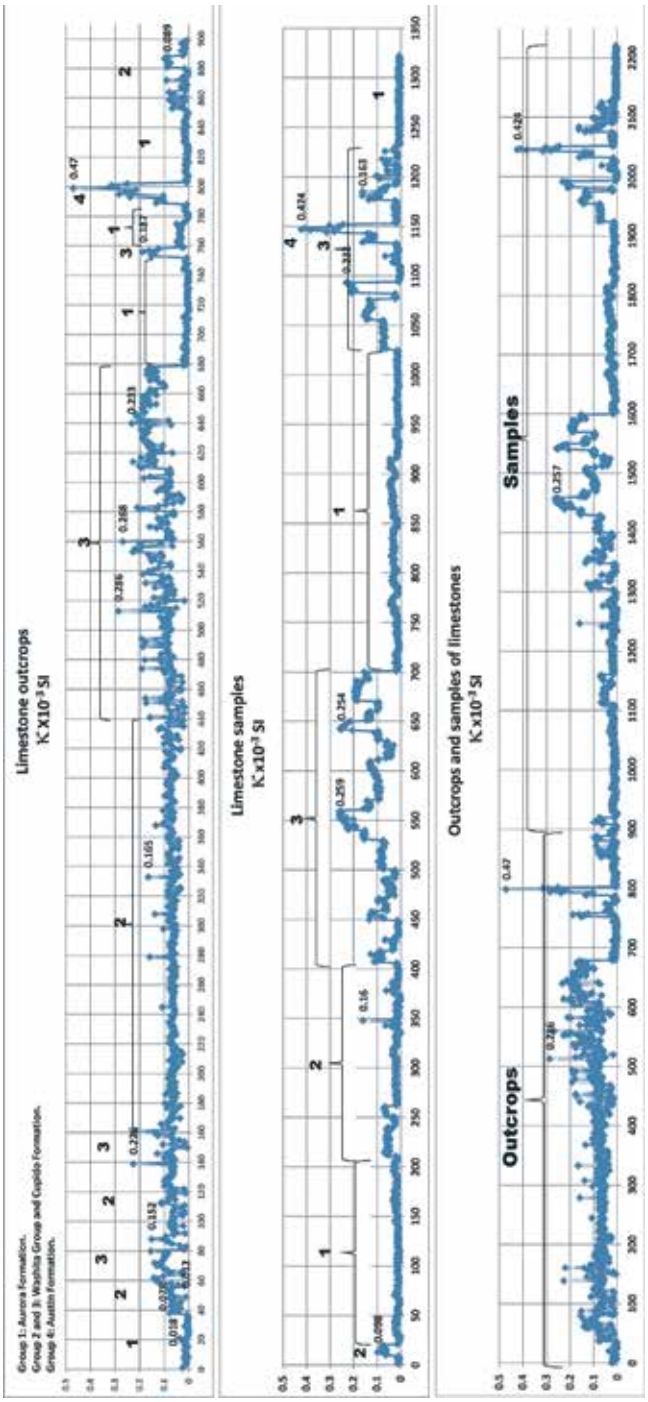

Figure 10. Variations of κ in limestones of the Sabinas basin. 1, 2 and 3 indicate groups of limestones according to values of κ.

Eagle Ford Formations. This group has κ higher and measurements are more varied than those in group 1, suggesting their formation was in unstable conditions in some areas of the basin in the Early Cretaceous during the deposition of the Cupido Formation.

Group 3 consists mainly of the Washita Group, characterized by higher κ and with greater variations than those recorded in groups 1 and 2. In this group, some measurements of the Taraises Formation are also located. The ages of these geological formations suggest two intervals of time with varying deposition conditions within the basin. The first interval is located at the beginning of Early Cretaceous (Taraises Formation) and the second interval at the beginning of Late Cretaceous (Washita Group; Fig. 2).

Group 4 has particular characteristics because it is composed of limestones of the Austin Formation which surrounds the Colorado intrusive, located near Monclova (Chávez-Cabello et al., 2011). The limestones in this group have the highest κ and greater variations with respect to the other groups. In other

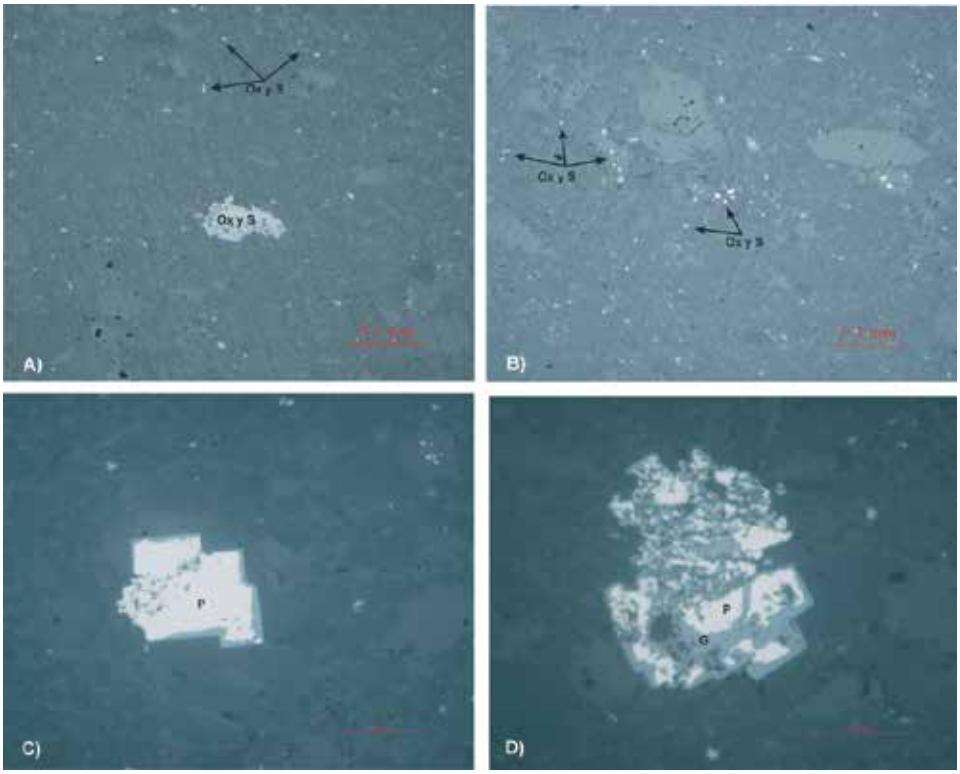

Figure 11. Thin sections in a sample of limestone belonging to Austin Formation intrude by igneous rocks (Colorado intrusive). RL-WA. *A*) and *B*): iron oxides and sulphides (Ox and S; light colors). *C*) Idiomorphic pyrite (P), slightly altered to goethite (G). *D*) Pyrite very altered to goethite.

outcrops far from the intrusive body, the geological formation (Austin Formation) has very low values of κ ($\leq 0.05 \times 10^{-3}$ SI), and in this case the geological formation is included in the group 1. The analysis of thin sections in a sample of limestone of the Austin Formation surrounding the Colorado intrusive reveals high enrichment in pyrite and iron oxides (Fig. 11). The pyrite has idiomorphic crystals indicating an epigenetic origin for these sulphides, *i.e.* added to the limestone probably from hydrothermal fluids during the emplacement of the intrusive body. Systematically, pyrite grains are altered to goethite. The amount and degree of alteration of pyrite determines the high values of κ recorded in the limestones belonging to group 4.

The separation into groups of limestones according to their ages of deposition and values of κ in the main geological formations to which they belong indicates variability in deposition environments of these rocks during the Cretaceous. These deposition environments determine different accumulations of magnetic minerals (paramagnetic and ferromagnetic minerals) in limestones. Apparently, such accumulations vary from place to place within the basin and are different in every geological formation.

The characteristics of the limestones in the studied region (Eguiluz de Antuñano, 2001; González-Sánchez et al., 2007), indicates that there are several possible causes for the high values of κ in the limestones of groups 2 and 3; *e.g.*, the formation of limestones in an anoxic or reducing environment (Merinero et al., 2010) and high siliciclastic content in limestones (Crick et al., 1997; Ellwood et al., 1999).

For the formation of limestones in an anoxic or reducing environment, the κ is related with darker limestones and, therefore, is richer in organic matter. During the accumulation and transformation of organic matter, sulphides (*e.g.* authigenic pyrites) are formed indicating bacterial activity (Merinero et al., 2010). Later these sulphides can be altered to iron oxides (*e.g.* magnetite) during the stage of diagenesis (Hladil et al., 2006). In this case, a change occurred in the valence state of Fe in the presence of oxygen, affecting some minerals such as pyrite and causing the formation of iron oxides and hydroxides (Dyussembayeva et al., 2014).

The analysis of thin sections in a sample of limestone belonging to Cupido Formation (Fig. 12) supports this first possible cause. This analysis indicates a dolomitic limestone with many iron oxides and framboidal pyrite. Generally, this latter mineral is transformed to iron oxides (*e.g.* magnetite and hematite). Some iron oxides are also transformed to other iron oxides and hydroxides (*e.g.* hematite and goethite). Framboidal pyrite is the result of bacterial reduction of seawater sulfates during diagenesis (Trudinger, 1981; Hall, 1986).

The high siliciclastic content in these limestones could indicate an increased supply of detritus to the basin due to a decrease in sea level and an increase in erosive activity (Crick et al., 1997; Ellwood et al., 1999). These processes can generate siliciclastic sediments enriched in paramagnetic minerals (*e.g.* clays,

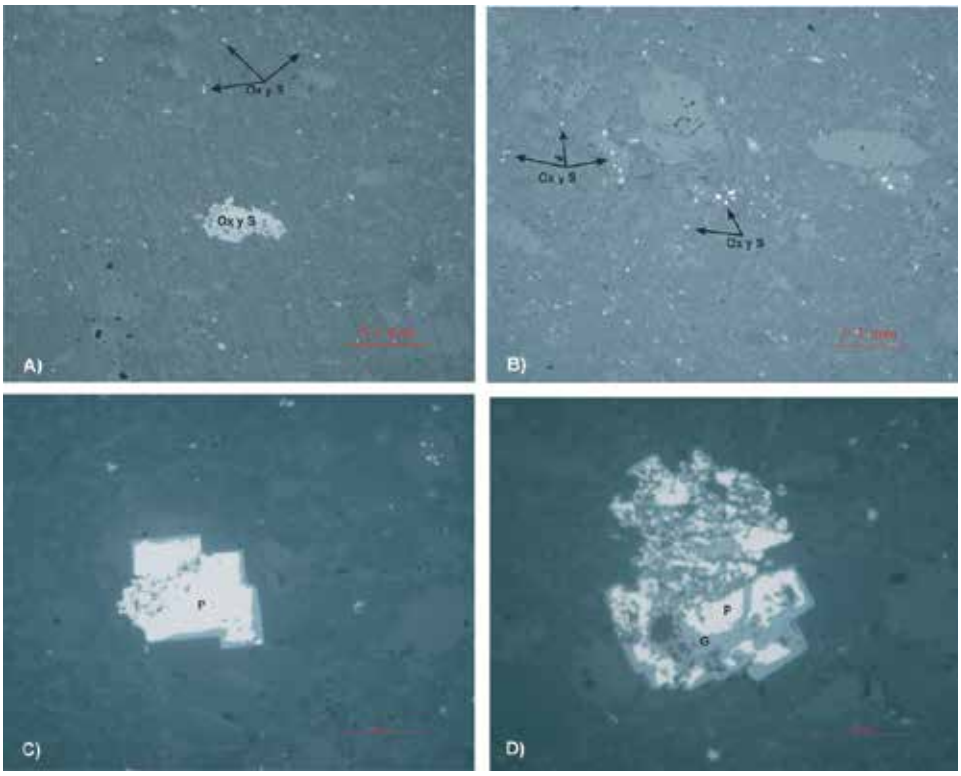

Figure 12. Thin sections in samples of limestone belonging to Cupido Formation (*A*, *B* and *C*) and Eagle Ford Formation (*D*). *A*) RL-WA: iron oxides (Ox; gray color) and pyrite grains with framboid texture (Py). *B*) TL-WA: transformation of iron oxides to goethite (G; indicated by arrows). *C*) RL-WA: framboids of pyrite altered to iron oxide (indicated by arrows). *D*) RL-A: framboidal pyrite (Py) which is transformed to iron oxides and hydroxides (mainly goethite; G).

chlorites, glauconites, micas, siderite and pyrite) and authigenic particles (Ellwood et al., 2000). In these groups, κ could be an indicator of siliciclastic supply due to fluctuations in weather and / or sea level (Crick et al., 2001). Some studied geological formations belonging to groups 2 and 3 (*e.g.* Eagle Ford and Taraise formations, and Washita Group) have limestones with high siliciclastic content, according to Eguiluz de Antuñano (2001) and González-Sánchez et al. (2007). The analysis of thin sections in a sample of limestone belonging to Eagle Ford Formation (Fig. 12) reveals framboidal pyrite, as well as iron oxides and hydroxides (*e.g.* goethite) generated from altering these sulphides.

The analysis of NGR in these limestones also suggests using this physical property as indirect proxy to characterize its mineralogical composition and its possible formation conditions.

The correlation matrix in samples of limestones indicates that the $I_{g,total}$ is related with the three radioelements, mainly with Th (Tab. 4). This supports the

idea of the presence of siliciclastic impurities and organic matter in these rocks. In this matrix, a negative relation between U and the others two radioelements is also observed. The U is likely related mainly with organic matter, whereas Th and K are generally related to the siliciclastic content (clays, micas, etc.) according to results obtained in other investigations (Lüning et al., 2004). Th and K are uncorrelated, therefore both radioelements may relate to different mineral phases within the siliciclastic fraction. The tendency to correlate the κ and $I_{g,total}$ suggests a probable relationship between the siliciclastic impurities of the limestones and κ. However, the noncorrelation of κ with Th and K indicates that in these impurities the fraction of ferromagnetic minerals contributes more than the fraction of paramagnetic minerals to the values of κ, according to the results obtained in similar rocks (Bábek et al., 2010).

6. Conclusions

From the analysis of the magnetic susceptibility (κ) and natural gamma radioactivity (NGR) in two types of sedimentary rocks (sandstone and limestone) of the Sabinas basin, it shows that these physical properties can be used as indirect proxies to carry out their characterization. Such physical properties are related to the mineral composition and degree alteration linked principally with the weathering. With the weathering process, high contents of Th and K, as well as high values of κ generated new mineral phases (clays, iron oxides and hydroxides). The relationship between this process and the physical properties is greater in sandstones, caused by the mineralogical composition. It is possible to divide the sandstones into three groups according to their values of κ indicating a high degree of magnetic heterogeneity, related to primary and secondary magnetic minerals. Generally, the primary magnetic minerals are found in the cement of these rocks and are comprised of iron oxides and hydroxides generated before and during the formation of the rocks, *i.e.*, derivative sources of sediments or formed in the early stages of diagenesis. The values of κ also are linked to the colorations of these rocks. Generally, the red sandstones have the highest content of primary and secondary magnetic minerals, though some gray-green sandstone show higher concentrations of secondary magnetic minerals.

The behavior of the NGR in the sandstones also indicates compositional heterogeneity. This physical property suggests that red colors on these rocks are not only linked with depositional conditions (diagenesis) but also with subsequent processes which cause alteration in surface conditions (weathering). Similarly, this physical property is related to other properties of the sandstones, such as hardness and grain sizes of minerals. From the analysis of the relationships among the radioelements, the sandstones also can be classified in terms of their composition, sources supply of sediments, degree of weathering and sediment transport. Also, it is possible to suggest which of

these rocks have higher contents of feldspar, quartz and clay-ferruginous cement. The clay content suggested by the relationships between the radioelements is not only related to late weathering processes, but also to a diagenetic process that determines the cement composition of the rock.

The classification of limestones into groups uses the values of κ and the analysis of this physical property and NGR, considers the stratigraphic position of limestones of different geological formations, and indicates variability in the deposition environments of these rocks during the Lower and Upper Cretaceous epochs. Those environments determine different compositions of paramagnetic and ferromagnetic minerals in the limestones belonging to such groups, principally in the Aurora, Cupido and Taraise Formations, as well as the Washita Group. The composition of magnetic minerals is different between geological formations belonging to the same groups and even within the same geological formation.

Acknowledgements – We thank the University Autonomous of Coahuila for its support of this research. Also thanks are granted to the Departament de Cristallografia, Mineralogia i Dipòsits Minerals de la Universitat de Barcelona for the access to the Optical Mineralogy Laboratory.

References

Adams, J. A. S. and Weaver, C. E. (1958): Thorium-to-uranium ratios as indicators of sedimentary processes; example of concept of geochemical facies, *Am. Assoc. Pet. Geol. Bull.*, **42**, 387–430.

Bábek, O., Kalvoda, J., Aretz, M., Cossey, P. J., Devuyst, F., Herbig, H. and Sevastopulo, G. (2010): The correlation potential of magnetic susceptibility and outcrop gamma-ray logs at Tournaisian-Viséan boundary sections in western Europe, *Geol. Belg.*, **13**, 291–308.

Banerje, A. and Banerjee, D. M. (2010): Modal analysis and geochemistry of two sandstones of the Bhander Group (Late Neoproterozoic) in parts of the Central Indian Vindhyan basin and their bearing on the provenance and tectonics, *J. Earth Syst. Sci.*, **119**, 825–839, DOI:10.1007/s12040-010-0056-z.

Bea, F. (1999): Uranium, in: *Encyclopedia of Geochemistry*, edited by Marshall, C. P. and Fairbridge, R. W. Kluwer Academic Publishers, London, 712 pp.

Boggs, S. (2009): *Petrology of Sedimentary Rocks*. 2nd edition. Cambridge University Press, Cambridge, England, 600 pp.

Chávez-Cabello, G., Aranda-Gómez, J. J. and Iriondo-Perrone, A. (2011): Culminación de la Orogenia Laramide en la Cuenca de Sabinas, Coahuila, México, *A. M. G. P., A.C.*, **56**, 80–91.

Chávez-Cabello, G., Aranda-Gómez, J. J., Molina-Garza, R. S., Cossío-Torres, T., Arvizu-Gutiérrez I. R. and González-Naranjo, G. A. (2005): La falla San Marcos: Una estructura jurásica de basamento multirreactivada del noreste de México, *B. Soc. Geol. Mex.,* **57**, 27–52.

Clark, D. A. (1997): Magnetic petrophysics and magnetic petrology: Aids to geological interpretation of magnetic surveys, *AGSO J. Aust. Geol. Geophys*, **17**, 83–103.

Corona-Esquivel, R., Tritlla, J., Benavides-Muñoz, M. E., Piedad-Sánchez, N. and Ferrusquía-Villafranca, I. (2006): Geología, estructura y composición de los principales yacimientos de carbón mineral en México, *B. Soc. Geol. Mex.,* **58**, 141–160.

Crick, R. E., Ellwood, B. B., Feist, R. and Hladil, J. (1997): Magnetosusceptibility event and cyclostratigraphy (MSEC) of the Eifelian-Givetian GSSP and associated boundary sequences in North Africa and Europe, *Episodes*, **20**, 167–175.

Crick, R. E., Ellwood, B. B., El Hassani, A., Hladil, J., Hrouda, F. and Chlupác, I. (2001): Magnetosusceptibility event and cyclostratigraphy (MSEC) of the Pridolian-Lochkovian GSSP (Klonk, Czech Republic) and coeval sequences in Anti-Atlas (Morocco), *Palaeogeogr. Palaeoclimatol. Palaeoecol.*, **167**, 73–100.

Dickson, B. L. and Scott, K. M. (1997): Interpretation of aerial gamma ray surveys-adding the geochemical factors, *AGSO J. Aust. Geol. Geophys.*, **17**, 187–200.

Dyussembayeva, K. Sh., Baitatsha, A. B., Kassenova, A. T. and Assubayeva, S. K. (2014): Micro- and nanogold in the auriferous of weathering crusts of Martovskoye and Ravninnoye deposits (west Kazakhstan), *Life Sci. J.*, **11**(5s), 263–266.

Eguiluz de Antuñano, S. (2001): Geologic evolution and gas resources of the Sabinas Basin in northeastern Mexico, in *The Western Gulf of Mexico Basin: Tectonics, Sedimentary Basins and Petroleum Systems*, edited by Bartolini, C., Buffler, R. T. and Cantú-Chapa, A. *AAPG Memoir*, **75**, 241–270.

Ellwood, B. B., Crick, R. E. and El Hassani, A. (1999): The magnetosusceptibility event and cyclostratigraphy (MSEC) method used in geological correlation of Devonian rocks from Anti-Atlas Morocco, *Am. Assoc. Pet. Geol. Bull.* **83**, 1119–1134.

Ellwood, B. B., Crick, R. E., El Hassani, A., Benoist, S. L. and Young, R. H. (2000): Magnetosusceptibility event and cyclostratigraphy method applied to marine rocks: detrital input versus carbonate productivity, *Geology*, **28**, 1135–1138.

García-Alonso, D., Canet, C., González-Partida, E., Villanueva-Estrada, R. E., Prol-Ledesma, R. M., Alfonso, P., Caballero-Martínez, J. A. and Lozano-Santa Cruz, R. (2011): The Cretaceous sediment-hosted copper deposits of San Marcos (Coahuila, Northeastern Mexico): An approach to ore-forming processes, *J. S. Am. Earth Sci.*, **31**, 432–443, DOI:10.1016/j.jsames.2011.02.012.

Gbadebo, A. M. (2011): Natural radionuclides distribution in the granitic rocks and soils of abandoned Quarry sites, Abeokuta, Southwestern Nigeria, *Asian J. Appl. Sci.*, **4**, 176–185, DOI:10.3923/ajaps.2011.176.185.

Goldhammer, R. K., Lehmann, P. J., Todd, R. G., Wilson, Ward, W. C. and Johnson, C. R. (1991): *Sequence Stratigraphy and Cyclostratigraphy of the Mesozoic of Sierra Madre Oriental, Northeast Mexico*. Field Guidebook, Huston, Texas and New Orlenans, Lousiana, Gulf Coast Section, SEPM (Society for Sedimentary Geology), 85 pp.

González-Sánchez, F., González-Partida, E., Canet, C., Atudorei, V., Alfonso, P., Morales-Puente, P., Cienfuegos-Alvarado, E. and González-Ruiz, L. (2017): Geological setting and genesis of stratabound barite deposits at Múzquiz, Coahuila in northeastern Mexico, *Ore Geol. Rev.*, **81**, 1184–1192, DOI:10.1016/j.oregeorev.2015.10.008.

González-Sánchez, F., Puente-Solís, R., González-Partida, E. and Camprubí, A. (2007): Estratigrafía del Noreste de México y su relación con los yacimientos estratoligados de fluorita, barita, celestina y Zn-Pb, *B. Soc. Geol. Mex.,* **59**, 43–62.

Hall, A. (1986): Pyrite-pyrrhotine redox reactions in nature, *Mineral. Mag.*, **50**, 223–229, DOI:10.1180/minmag.1986.050.356.05.

Hladil, J., Gersl, M., Strnad, L., Frana, J., Langrova, A. and Spisiak, J. (2006): Stratigraphic variation of complex impurities in platform limestones and possible significance of atmospheric dust: a study with emphasis on gamma-ray spectrometry and magnetic susceptibility outcrop logging (Eifelian-Frasnian, Moravia, Czech Republic), *Int. J. Earth Sci.*, **95**, 703–723, DOI:10.1007/s00531-005-0052-8.

Imlay, W. R. (1936): Geology of the western part of the Sierra de Parras, *Geol. Soc. Am. Bull.*, **47**, 1091–1152, DOI:10.1130/GSAB-47-1091.

Krutak, P. R. (1965): Source areas of Patula Arkosa (Lower Cretaceous) Coahuila, Mexico: Notes, *J. Sediment. Petrol.*, **35**, 512–518.

Lüning, S., Wendt, J., Belka, Z. and Kaufmann, B. (2004): Temporal-spatial reconstruction of the early Frasnian (Late Devonian) anoxia in NW Africa: New field data from the Ahnet Basin (Algeria), *Sediment. Geol.*, **163**, 237–264, DOI:10.1016/S0037-0738(03)00210-0.

Merinero, R., Lunar, R. and Martínez, J. (2010): Carbonatos metanógenos y pirita framboidal autigénica: geomarcadores de la actividad de organismos quimiosintéticos en el Golfo de Cádiz, *Macla*, **12**, 29–37.

Mittlefehldt, D. W. (1999): Potassium, in: *Encyclopedia of Geochemistry*, edited by Marshall, C. P. and Fairbridge, R. W. Kluwer Academic Publishers, London, 712 pp.

Murillo-Muñeton, G. (1999): *Stratigraphic architecture, platform evolution, and mud-mound development in the Lower Cupido Formation (Lower Cretaceous), northeastern Mexico*, Ph.D. Dissertation, Texas A & M University, College Station, 53 pp.

Ocampo-Díaz, Y. Z. E., Talavera-Mendoza, O., Jenchen, U., Valencia, V. A., Medina-Ferrusquia, H. C. and Guerrero-Suastegui, M. (2014): Procedencia de la Formación La Casita y la Arcosa Patula: Implicaciones para la evolución tectono-magmática del NE de México entre el Carbonífero y el Jurásico, *Rev. Mex. Cienc. Geol.*, **31**, 45–63.

Pascacio-Toledo, R. (2001): Texto guía Carta magnética de Nueva Rosita G14-1. Escala 1:250,000, CRM, 19 pp.

Schuler, U., Erbe, P., Zarei, M., Rangubpit, W., Surinkum, A., Stahr, K. and Herrmann, L. (2011): A gamma-ray spectrometry approach to field separation of illuviation-type WRB reference soil groups in northern Thailand, *J. Plant. Nutr. Soil Sci.*, **174**, 536–544.

Trudinger, P. A. (1981): Origin of sulphide in sediments. BμR, *J. Austral. Geol. & Geophys.*, **6**, 279–285.

Tucker, M. E. (2003): *Sedimentary Rocks in the Field*. Third edition, Wiley, 234 pp.

Zand-Moghadam, H., Moussavi-Harami, R., Mahboubi, A. and Rahimi, B. (2013): Petrography and geochemistry of the early-middle Devonian sandstones of the Padeha Formation in the north of Kerman, SE Iran. Implications for provenance, *Bol. Inst. Fisiogr. Geol.*, **83**, 1–14.

Wilson, J. L. and Pialli, G. (1977): A Lower Cretaceous shelf margin in Northern Mexico, in: *Cretaceous Carbonates of Texas and Mexico: Applications to Subsurface Exploration*. The University of Texas at Austin, Bureau of Economic Geology, Report of Investigations, **89**, 286–298.

SAŽETAK

Magnetska susceptibilnost i prirodna gama radioaktivnost kao neizravni faktori za karakterizaciju pješčenjaka i vapnenaca zavalja Sabinas

José A. Batista Rodríguez, Joaquín A. Proenza Fernández, Antonio Rodríguez Vega, Felipe de Jesus López Saucedo i Karla I. Cázares Carreón

U radu je prikazana analiza magnetske susceptibilnosti i prirodne gama radioaktivnosti kao neizravnih faktora svojstava pješčenjaka i vapnenca zavalja Sabinas. Ove se stijene nalaze u sedimentnom slijedu, od gornje jure do krede. Magnetska susceptibilnost ukazuje na promjene u magnetskom sastavu ovih stijena i upućuje na promjene u stupnju njihovog trošenja. Raspon vrijednosti magnetske susceptibilnosti u pješčenjaku i

vapnencu omogućuje njihovo razvrstavanje u različite skupine, što upućuje na promjenljivost obzirom na uvjete nastanka i evolucije. Visoke vrijednosti magnetske susceptibilnosti u vapnencima mogu se povezati sa sedimentacijom u anoksičnom ili reduktivnom okolišu, kao i siliciklastičnim sadržajem. Prirodna gama-radioaktivnost izražena u sadržaju torija (Th) i omjeru koncentracija urana i kalija (U / K) te torija i urana (Th / U) također upućuju na stupanj trošenja tih stijena, uglavnom u pješčenjacima. Ovi odnosi ukazuju i na druge karakteristike pješčenjaka vezane uz vjerojatno podrijetlo sedimenata, njegovu udaljenost od izvorišta, stupanj trošenja i dinamiku transporta. Koristeći vrijednosti omjera U / K u pješčenjacima moguće je predložiti vjerojatne proporcije kvarca i feldspata. Temeljem ovih vrijednosti omogućena je klasifikacija stijena kao arkoza ili kvarcarenit, a što ukazuje na zrelost pješčenjaka. Prema vrijednostima omjera U / K većina tih stijena, koji pokazuju malu zrelost, zovu se arkoze. Koristeći vrijednosti Th / U omjera moguće je predložiti teksture kvarcarenita, klasificirajući ih kao klast potporne stijene ili one s matriksom.

Ključne riječi: magnetska susceptibilnost, prirodna gama radioaktivnost, vapnenci, pješčenjaci, zavalje Sabinas

Corresponding author's address: José A. Batista Rodríguez, Escuela Superior de Ingeniería, Universidad Autónoma de Coahuila, Blvd. Lic. Adolfo López Mateos s /n, Col. Independencia. Nueva Rosita, Coahuila. México, C. P. 26800; e-mail: josebatista@uadec.edu.mx